Finite-Element Solution of Planar Inhomogeneous Waveguides for Magnetostatic Waves

YI LONG, MASANORI KOSHIBA, SENIOR MEMBER, IEEE, AND MICHIO SUZUKI, SENIOR MEMBER, IEEE

***Abstract*—A unified numerical approach based on the finite-element method is described for the solution of planar inhomogeneous waveguides for magnetostatic waves. Both magnetostatic volume wave and magnetostatic surface wave modes are treated. The validity of the method is confirmed by calculating the magnetostatic wave modes of layered YIG films. The numerical results of inhomogeneous YIG films with α-power magnetization profile are also presented, and the effects of magnetization inhomogeneities on the delay characteristics and potential profiles for magnetostatic forward volume wave, magnetostatic backward volume wave, and magnetostatic surface wave modes are examined.**

I. Introduction

RECENTLY, MUCH attention has been paid to magnetostatic wave (MSW) modes in various complicated structures such as multilayered and inhomogeneous films to improve the delay characteristics [1]–[19]. Multilayer structures [1], [6], [10], [11], [13], [15] can be viewed as special cases of an arbitrary thickness variation of the magnetization M_s. The problem of arbitrary inhomogeneities cannot be easily attacked by classical boundary value techniques. Consequently, the variational method has been introduced for analyzing nonuniform geometries [7], [14], [16]–[19]. This method is valid for the solution of arbitrary magnetization profiles. However, great care is necessary in choosing the trial functions for fast convergence of the numerical solutions.

In this paper, a unified numerical approach based on the finite-element method is described for the solution of planar inhomogeneous waveguides for MSW modes. Both magnetostatic volume wave (MSVW) and magnetostatic surface wave (MSSW) modes are treated. In the finite-element method, the cross section of the planar waveguide is divided into line elements [20], [21] and it is easy to consider the variations in M_s. Therefore, the finite-element method enables one to compute easily and accurately the delay characteristics and potential profiles of the planar arbitrarily inhomogeneous MSW waveguides. The validity of the method is confirmed by calculating MSW modes of layered YIG films. The numerical results of inhomogeneous YIG films with α-power magnetization profile are also presented, and the effects of magnetization inhomogeneities on the delay characteristics and potential profiles for magnetostatic forward volume wave (MSFVW), magnetostatic backward volume wave (MSBVW), and MSSW modes are examined.

Manuscript received November 20, 1986; revised April 8, 1987.

The authors are with the Department of Electronic Engineering, Hokkaido University, Sapporo, 060 Japan.

IEEE Log Number 8715415.

II. Basic Equations

We consider a multilayered inhomogeneous waveguide for MSW modes as shown in Fig. 1(a), where each ferrite film has an arbitrary thickness variation of the magnetization M_s. When the bias field H_0 is applied in parallel with the x, y, and z directions, MSFVW, MSBVW, and MSSW modes propagate along the y direction, respectively.

The constitutive relations are

$$\boldsymbol{B} = \mu_0[\mu_r]\boldsymbol{H} \qquad \text{for ferrite} \tag{1a}$$

$$\boldsymbol{B} = \mu_0\boldsymbol{H} \qquad \text{for dielectric} \tag{1b}$$

where $\boldsymbol{B}$ is the magnetic flux density vector, $\boldsymbol{H}$ is the magnetic field vector, μ_0 is the permeability in free space, and $[\mu_r]$ is the relative permeability tensor.

With a time dependence of the form $\exp(j\omega t)$ being implied, $[\mu_r]$ takes the form

$$[\mu_r] = \begin{bmatrix} 1 & 0 & 0 \\ 0 & \mu & j\kappa \\ 0 & -j\kappa & \mu \end{bmatrix} \qquad \text{for MSFVW} \tag{2a}$$

$$[\mu_r] = \begin{bmatrix} \mu & 0 & -j\kappa \\ 0 & 1 & 0 \\ j\kappa & 0 & \mu \end{bmatrix} \qquad \text{for MSBVW} \tag{2b}$$

$$[\mu_r] = \begin{bmatrix} \mu & j\kappa & 0 \\ -j\kappa & \mu & 0 \\ 0 & 0 & 1 \end{bmatrix} \qquad \text{for MSSW} \tag{2c}$$

where

$$\mu = \frac{\omega_i(\omega_i + \omega_m) - \omega^2}{\omega_i^2 - \omega^2} \tag{3a}$$

$$\kappa = \frac{\omega_m \omega}{\omega_i^2 - \omega^2}. \tag{3b}$$

Here $\omega_i = -\gamma\mu_0 H_i$, $\omega_m = -\gamma\mu_0 M_s$, γ is the gyromagnetic ratio, and H_i is the internal magnetic field in the ferrimagnetic film; $H_i = H_0 - M_s$ for MSFVW and $H_i = H_0$ for MSBVW and MSSW.

0018-9480/87/0800-0731$01.00 ©1987 IEEE

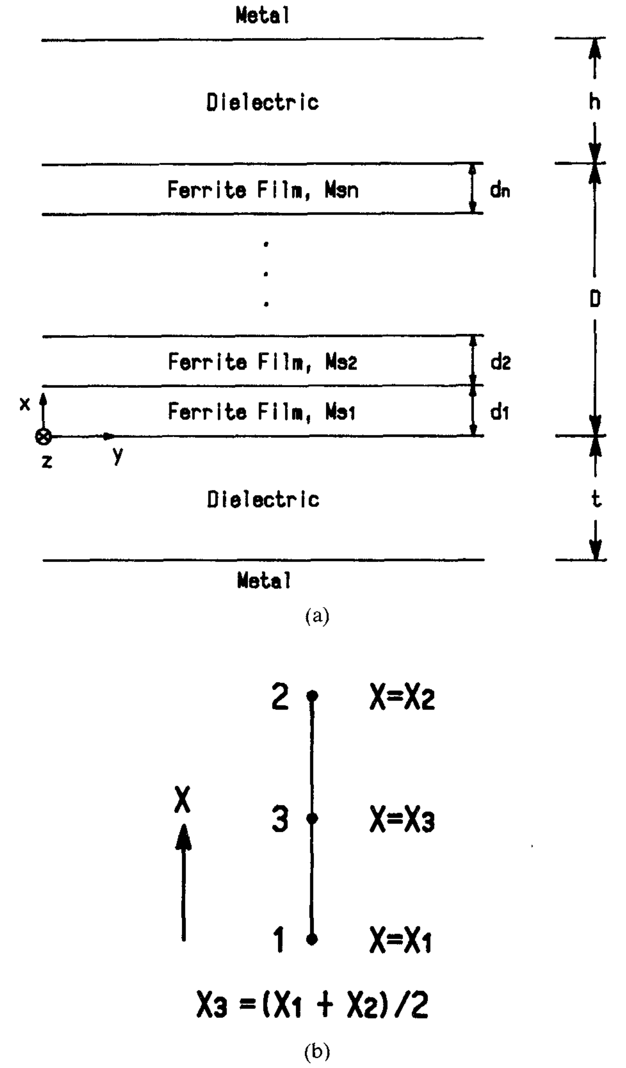

Fig. 1. (a) Geometry of a planar MSW waveguide. (b) Line element

Assuming that there is no variation of all fields in the z direction, from Maxwell's equations and the magnetostatic approximation condition, the following basic equations for MSW waveguides are obtained:

$$\partial B_x/\partial x - js\beta B_y = 0 \tag{4}$$

$$H_x = -\partial\phi/\partial x \tag{5a}$$

$$H_y = js\beta\phi \tag{5b}$$

where β is the phase constant in the y direction, $s = \pm 1$ is a directional parameter [17], and ϕ is the magnetostatic potential.

III. Mathematical Formulations

A. Finite-Element Approach

Dividing the region $0 \leqslant x \leqslant D$ into a number of second-order line elements [20], [21] as shown in Fig. 1(b), the magnetic potential ϕ within each element is defined in terms of the magnetic potentials ϕ_1 to ϕ_3 at the nodal points 1 to 3, as follows:

$$\phi = \{N\}^T\{\phi\}_e \exp(-js\beta y) \tag{6}$$

where

$$\{\phi\}_e = [\phi_1 \quad \phi_2 \quad \phi_3]^T \tag{7}$$

$$\{N\} = [N_1 \quad N_2 \quad N_3]^T. \tag{8}$$

Here T, $\{\cdot\}$, and $\{\cdot\}^T$ denote a transpose, a column vector, and a row vector, respectively, and the shape functions $N_1 - N_3$ are given by

$$N_1 = L_1(2L_1 - 1) \tag{9a}$$

$$N_2 = L_2(2L_2 - 1) \tag{9b}$$

$$N_3 = 4L_1L_2 \tag{9c}$$

where

$$L_1 = (x_2 - x)/(x_2 - x_1) \tag{10a}$$

$$L_2 = (x - x_1)/(x_2 - x_1). \tag{10b}$$

Using a Galerkin procedure on (4), we obtain

$$\int_{x_1}^{x_2} \{N\}(\partial B_x/\partial x - js\beta B_y)\, dx = \{0\} \tag{11}$$

where $\{0\}$ is a null vector.

Integrating by parts, (11) becomes

$$\int_{x_1}^{x_2} (-\{N_x\}B_x - js\beta\{N\}B_y)\, dx + [B_x]_{x=x_1}^{x=x_2} = \{0\} \tag{12}$$

where $\{N_x\} = d\{N\}/dx$.

Noting (1), (2), (5), and (6) and assembling the complete matrix for the region $0 \leqslant x \leqslant D$ by adding the contributions of all different elements, the following global matrix equation is derived:

$$[A]\{\phi\} - B_0/\mu_0 + B_D/\mu_0 = \{0\} \tag{13}$$

where

$$[A] = \sum_e \int_{x_1}^{x_2} \left[\{N_x\}\{N_x\}^T + \mu_e\beta^2\{N\}\{N\}^T\right] dx \qquad \text{for MSFVW} \tag{14a}$$

$$[A] = \sum_e \int_{x_1}^{x_2} \left[\mu_e\{N_x\}\{N_x\}^T + \beta^2\{N\}\{N\}^T\right] dx \qquad \text{for MSBVW} \tag{14b}$$

$$[A] = \sum_e \int_{x_1}^{x_2} \left[\mu_e\{N_x\}\{N_x\}^T + \mu_e\beta^2\{N\}\{N\}^T + s\kappa_e\beta\left(\{N_x\}\{N\}^T + \{N\}\{N_x\}^T\right)\right] dx \qquad \text{for MSSW.} \tag{14c}$$

Here the components of $\{\phi\}$ vector are the values of ϕ at the nodal points in the region $0 \leqslant x \leqslant D$. B_0 and B_D are the values of B_x at the nodal points on $x = 0$ and $x = D$, respectively, and Σ_e extends over all different elements.

B. Analytical Solution in Dielectric

Considering $B_x = 0$ at $x = -t$ and $x = D + h$, we obtain the following analytical solutions for the dielectric regions:

$$\phi = \begin{cases} \phi_- \cosh\beta(x+t)\exp(-js\beta y), & -t \leqslant x \leqslant 0 \\ \phi_+ \cosh\beta(x - D - h)\exp(-js\beta y), & D \leqslant x \leqslant D + h \end{cases} \tag{15}$$

TABLE I
CONVERGENCE BEHAVIOR IN CALCULATION OF β FOR MSW MODES OF HOMOGENEOUS WAVEGUIDES

modes	f(GHz)	N_E	$\frac{\lvert \beta_{exact} - \beta_{FEM} \rvert}{\beta_{exact}}$ (%)
MSFVW	2.85	1	0.00047
	2.95	1	0.00167
		2	0.00024
		4	0.00015
	3.05	1	0.00500
		2	0.00042
		4	0.00001
	3.23	1	0.01315
		2	0.00131
		4	0.00006
MSBVW	2.00	2	0.13716
		4	0.00856
		5	0.00351
	2.50	2	0.02533
		4	0.00157
		5	0.00064
	2.80	2	0.00178
		4	0.00011
		5	0.00005
MSSW (s=1)	2.20	1	0.000003
	2.60	1	0.00069
		2	0.00005
		3	0.00001
		4	0.000005
	2.90	1	0.43333
		2	0.02788
		3	0.00555
		4	0.00176
MSSW (s=-1)	2.20	1	0.00008
	2.60	1	0.00861
		2	0.00054
		3	0.00011
		4	0.00003
	2.90	1	0.41790
		2	0.02699
		3	0.00538
		4	0.00171

$$B_x = \begin{cases} -\mu_0 \beta \phi_- \sinh \beta(x+t) \exp(-js\beta y), \\ \quad -t \leqslant x \leqslant 0 \\ -\mu_0 \beta \phi_+ \sinh \beta(x-D-h) \exp(-js\beta y), \\ \quad D \leqslant x \leqslant D+h \end{cases} \tag{16}$$

where ϕ_+ and ϕ_- are arbitrary constants.

From (15) and (16) we obtain

$$B_0/\phi_0 = -\mu_0 \beta \tanh \beta t \tag{17a}$$

$$B_D/\phi_D = \mu_0 \beta \tanh \beta h \tag{17b}$$

where ϕ_0 and ϕ_D are the values of ϕ at the nodal points $x=0$ and $x=D$, respectively.

C. Combination of Finite-Element and Analytical Relations

Substituting (17) into (13), we obtain the following final matrix equation:

$$[A]\{\phi\} + \phi_0 \beta \tanh \beta t + \phi_D \beta \tanh \beta h = \{0\}. \tag{18}$$

This equation determines the propagation characteristics for various MSW modes.

IV. COMPUTED RESULTS

As a test for the numerical accuracy of the method proposed here, we consider layered structures [1], [6], [10], [11], [13], [15]. In the MSFVW case, consider a triple-layered YIG film structure with $M_{s1}=1750$ G, $d_1=90$ μm, $M_{s2}=1500$ G, $d_2=10$ μm, $M_{s3}=1680$ G, $d_3=7$ μm, $h=127$ μm, and $t \to \infty$. In the MSBVW case, consider a single film with $M_s=1200$ G, $d=30$ μm, and $h=635$ μm, and $t \to \infty$. In the MSSW case, consider a single-film with $M_s=1750$ G, $d=10$ μm, $h=25$ μm, and $t \to \infty$. Table I shows the relative error $|\beta_{exact} - \beta_{FEM}|/\beta_{exact}$, where β_{exact} and β_{FEM} are the exact solutions and the finite-element solutions, respectively, and N_E is the number of the line elements. By using a few elements, a rapid convergence can be obtained. In the MSFVW and MSSW cases, the solutions near the upper cutoff frequency have a slower convergence behavior. In the MSBVW case, on the other hand, the solutions near the lower cutoff frequency have a slower convergence behavior.

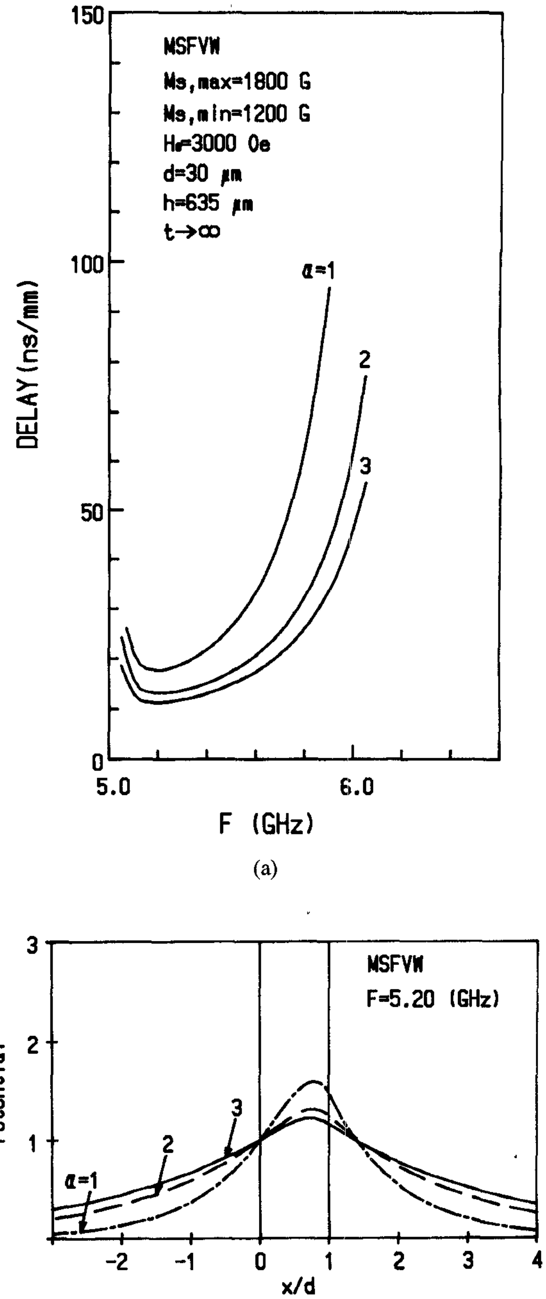

Fig. 2. MSFVW modes. (a) Delay characteristics. (b) Potential profiles.

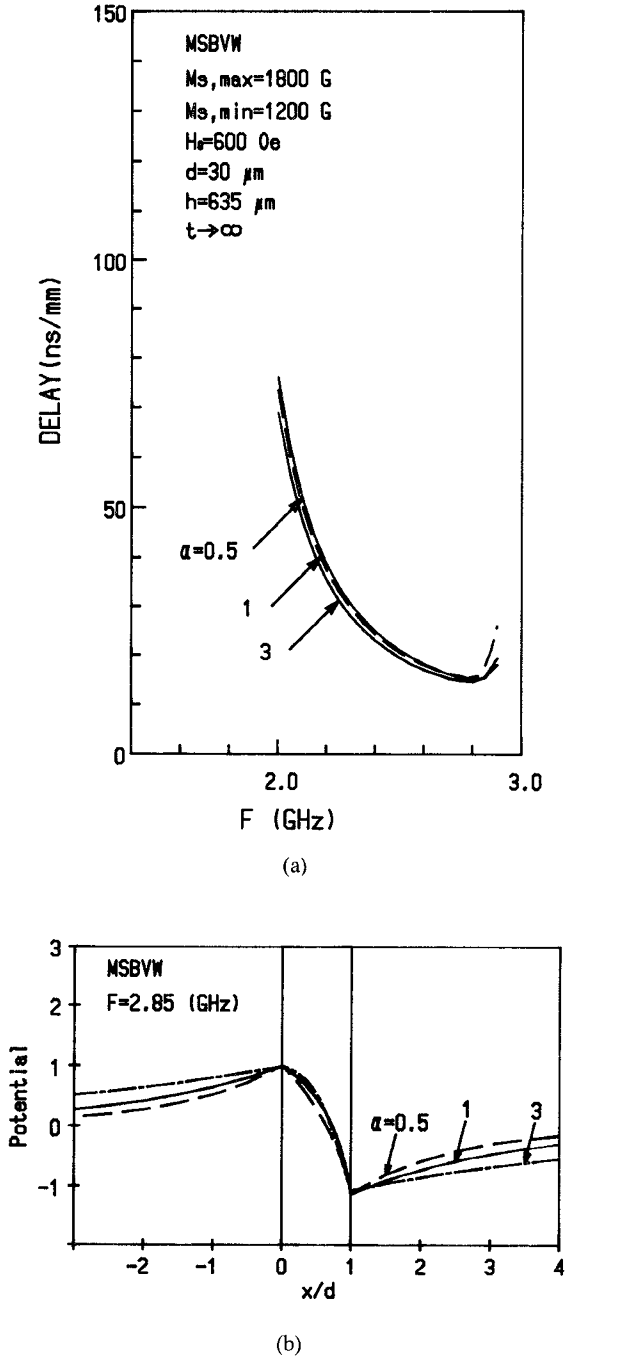

Fig. 3. MSBVW modes. (a) Delay characteristics. (b) Potential profiles.

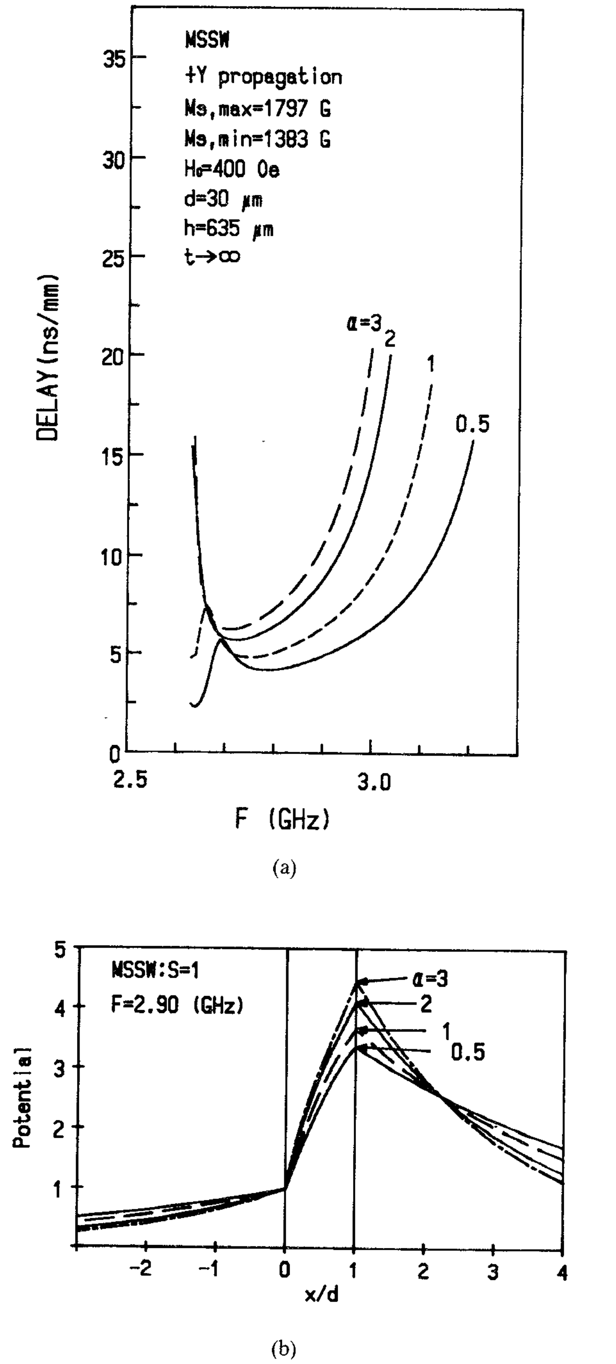

Fig. 4. MSSW modes propagating in the positive y direction ($s=1$). (a) Delay characteristics. (b) Potential profiles.

As the numerical examples, we consider a single YIG film with α-power magnetization profile, $d = 30$ μm, $h = 635$ μm, and $t \to \infty$. The magnetization M_s is given by

$$M_s = M_{s,\min} + (M_{s,\max} - M_{s,\min})[(d-x)/d]^{\alpha} \quad (19)$$

where $M_{s,\max}$ and $M_{s,\min}$ are the maximum and minimum values of M_s, respectively.

Fig. 2(a) shows the group delay for MSFVW modes, where $M_{s,\max} = 1800$ G, $M_{s,\min} = 1200$ G, and $H_0 = 3000$ Oe. The potential profiles at $f = 5.2$ GHz are given in Fig. 2(b). The delay curves depend on the values of α. As the α value becomes small, the group delay increases and the potential has a stronger localization near a film surface.

Fig. 3(a) shows the group delay for MSBVW modes, where $M_{s,\max} = 1800$ G, $M_{s,\min} = 1200$ G, and $H_0 = 600$ Oe. The potential profiles at $f = 2.85$ GHz are given in Fig. 3(b). The delay curves are not sensitive to the α value.

Figs. 4(a) and 5(a) show the group delay for MSSW modes propagating in the positive ($s = 1$) and negative ($s = -1$) y directions, respectively, where $M_{s,\max} = 1797$ G, $M_{s,\min} = 1383$ G, and $H_0 = 400$ Oe. The potential profiles for both MSSW modes at $f = 2.9$ GHz are given in Figs. 4(b) and 5(b). In the case $s = 1$, as the α

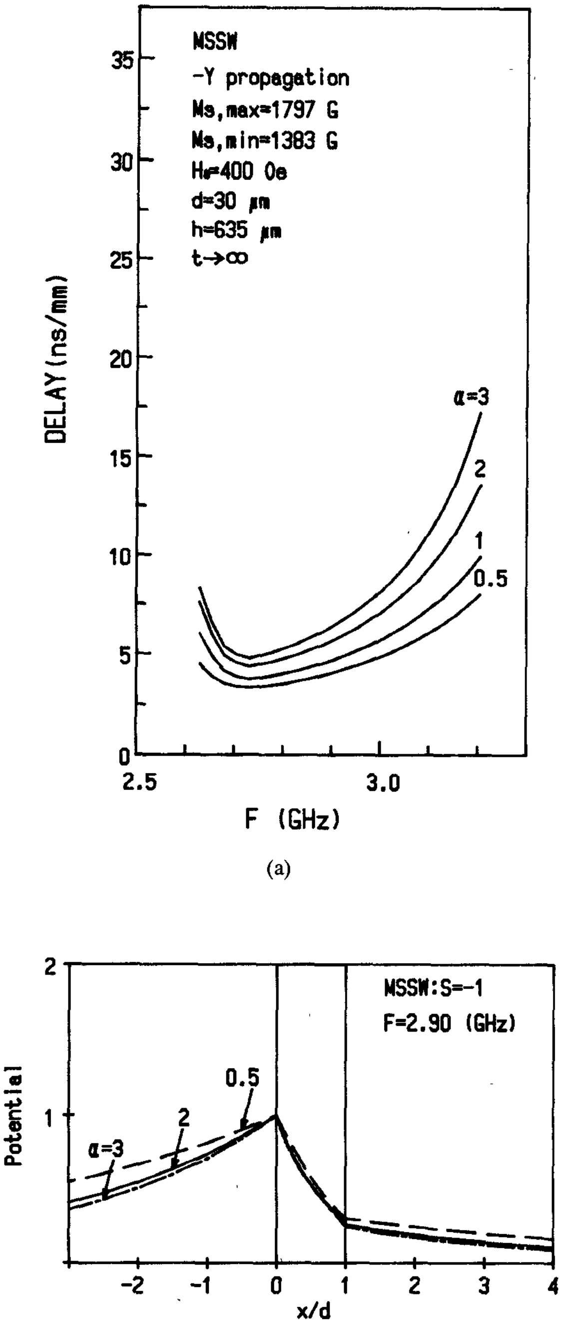

(b)

Fig. 5. MSSW modes propagating in the negative y direction ($s = -1$). (a) Delay characteristics. (b) Potential profiles.

value becomes large, the delay peak moves toward lower frequencies. This effect is similar to that obtained by varying the dielectric thickness of the dielectric layered homogeneous MSSW waveguide [1].

It is found from Figs. 2–5 that by changing the α value, the group delay can be controlled and that a further improvement in bandwidth for nondispersive MSW propagation may be achieved using optimized magnetization profiles.

In the above calculation, 19 elements are used. When the convergence of the solution is not sufficient, the number of elements is increased. Table II shows the convergence behavior, where β_{19} and β_{29} are the values of β obtained by using 19 and 29 elements, respectively. The convergence is dependent on the α value.

TABLE II
CONVERGENCE BEHAVIOR IN CALCULATION OF β FOR MSW MODES OF INHOMOGENEOUS WAVEGUIDES

modes	α	f(GHz)	$\frac{\lvert\beta_{29} - \beta_{19}\rvert}{\beta_{29}}$ (%)
MSFVW	1	5.10 5.25 5.70	0.12517 0.00202 0.00006
	2	5.10 5.30 5.70	0.00005 0.000008 0.00002
	3	5.15 5.50 5.85	0.000000 0.000000 0.000000
MSBVW	0.5	2.10 2.50 2.90	0.00351 0.01658 0.25430
	1	2.10 2.50 2.90	0.00002 0.000002 0.27022
	3	2.10 2.50 2.90	0.000009 0.000005 0.000330
MSSW (s=1)	0.5	2.63 2.83 3.03	0.06940 0.01188 0.01797
	1	2.63 2.83 3.03	0.43200 0.000003 0.000000
	2	2.63 2.83 3.03	2.24659 0.00003 0.000009
	3	2.63 2.83 3.03	3.67759 0.00014 0.00005
MSSW (s=-1)	0.5	2.63 2.83 3.03	0.06544 0.00685 0.00644
	1	2.63 2.83 3.03	0.34885 0.000007 0.000008
	2	2.63 2.83 3.03	1.13832 0.00007 0.00003
	3	2.63 2.83 3.03	1.78663 0.00027 0.00006

V. CONCLUSIONS

A finite-element method was developed for the analysis of planar inhomogeneous waveguides for MSW modes. Both MSVW and MSSW modes are treated in a unified manner. In this approach, the nonphysical spurious solutions do not appear. The validity of the method is confirmed by calculating MSW modes of layered YIG films. The numerical results of inhomogeneous YIG films with α-power magnetization profile are also presented, and the effects of magnetization inhomogeneities on the delay characteristics and potential profiles for MSFVW, MSBVW, and MSSW modes are examined.

This method may be extended to three-dimensional inhomogeneous MSW waveguides [7], [16].

REFERENCES

[1] W. L. Bongianni, "Magnetostatic propagation in a dielectric layered structure," *J. Appl. Phys.*, vol. 43, pp. 2541–2548, June 1972.

[2] D. A. Zeskind and F. R. Morgenthaler, "Located high-*Q* ferromagnetic resonance in nonuniform magnetic fields," *IEEE Trans. Magn.*, vol. MAG-13, pp. 1249–1251, Sept. 1977.

[3] F. R. Morgenthaler, "Magnetostatic waves bound to dc field gradient," *IEEE Trans. Magn.*, vol. MAG-13, pp. 1252–1254, Sept. 1977.
[4] F. R. Morgenthaler, "Bound magnetostatic waves controlled by field gradients in YIG single crystals and epitaxial films," *IEEE Trans. Magn.*, vol. MAG-14, pp. 806–810, Sept. 1978.
[5] T. Ohira, M. Tsutsumi, and N. Kumagai, "The magnetostatic surface waves propagating through a YIG magnetized in the raised cosine profile" (in Japanese), *Trans. Inst. Electron. Commun. Eng. Jap.*, vol. J62-B, pp. 603–604, June 1979.
[6] L. R. Adkins and H. L. Glass, "Dispersion control in magnetostatic delay lines by means of multiple magnetic layer structure," in *1980 Ultrason. Sym. Proc.*, 1980, pp. 526–531.
[7] M. Tsutsumi, Y. Masaoka, T. Ohira, and N. Kumagai, "A new technique for magnetostatic wave delay lines," *IEEE Trans. Microwave Theory Tech.*, vol. MTT-29, pp. 583–587, June 1981.
[8] C. H. Wilts and S. Prasad, "Determination of magnetic profiles in implanted garnets using ferromagnetic resonance," *IEEE Trans. Magn.*, vol. MAG-17, pp. 2405–2414, Sept. 1981.
[9] R. L. Carter, J. M. Owens, C. W. Smith, and K. W. Reed, "Ion-implanted magnetostatic wave reflective array filters," *J. Appl. Phys.*, vol. 53, pp. 2655–2657, Mar. 1982.
[10] M. R. Daniel and P. R. Emtage, "Magnetostatic volume wave propagation in a ferromagnetic double layer," *J. Appl. Phys.*, vol. 53, pp. 3723–3729, May 1982.
[11] J. P. Parekh and K. W. Chang, "MSFVW dispersion control utilizing a layered YIG-film structure," *IEEE Trans. Magn.*, vol. MAG-18, pp. 1610–1612, Nov. 1982.
[12] D. D. Stancil and F. R. Morgenthaler, "Guiding magnetostatic surface waves with nonuniform in-plane fields," *J. Appl. Phys.*, vol. 54, pp. 1613–1618, Mar. 1983.
[13] J. P. Parekh and K. W. Chang, "Nondispersive magnetostatic-forward-volume-wave propagation double-layered YIG-film structure," *Proc. IEEE*, vol. 71, pp. 685–686, May 1983.
[14] D. D. Stancil, "Variational formulation of magnetostatic wave dispersion relations," *IEEE Trans. Magn.*, vol. MAG-19, pp. 1865–1867, Sept. 1983.
[15] J. P. Parekh and K. W. Chang, "Nondispersive MSFVW propagation in a triple-YIG-film-layered structure," *IEEE Trans. Magn.*, vol. MAG-19, pp. 1868–1870, Sept. 1983.
[16] E. Sawado and N. S. Chang, "Variational approach to analysis of propagation of magnetostatic waves in highly inhomogeneously magnetized media," *J. Appl. Phys.*, vol. 55, pp. 1062–1067, Feb. 1984.
[17] N. E. Buris and D. D. Stancil, "Magnetostatic surface-wave propagation in ferrite thin films with arbitrary variations of the magnetization through the film thickness," *IEEE Trans. Microwave Theory Tech.*, vol. MTT-33, pp. 484–491, June 1985.
[18] N. E. Buris and D. D. Stancil, "Magnetostatic volume modes of ferrite thin films with magnetization inhomogeneities through the film thickness," *IEEE Trans. Microwave Theory Tech.*, vol. MTT-33, pp. 1089–1096, Oct. 1985.
[19] F. R. Morgenthaler, "Control of magnetostatic waves in thin films by means of spatially nonuniform bias fields," *Circuits Syst. Signal Process.*, vol. 4, pp. 63–88, 1985.
[20] O. C. Zienkiewitz, *The Finite Element Method*, 3rd ed. London: McGraw-Hill, 1977.
[21] M. Koshiba and M. Suzuki, "Numerical analysis of planar arbitrarily anisotropic diffused optical waveguides using finite-element method," *Electron. Lett.*, vol. 18, pp. 579–581, June 1982.

Yi Long was born in Nanchang, China, on December 1, 1955. She received the B.S. and M.S. degrees in electronic engineering from Huazhong University of Science and Technology, Wuhan, China, in 1982 and 1984, respectively. She is presently studying toward the Ph.D. degree in electronic engineering at Hokkaido University, Sapporo, Japan.

Ms. Long is a member of the Institute of Electronics and Communication Engineers of Japan.

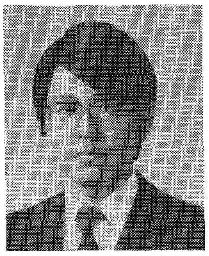

Masanori Koshiba (SM'84) was born in Sapporo, Japan, on November 23, 1948. He received the B.S., M.S., and Ph.D. degrees in electronic engineering from Hokkaido University, Sapporo, Japan, in 1971, 1973, and 1976, respectively.

In 1976, he joined the Department of Electronic Engineering, Kitami Institute of Technology, Kitami, Japan. Since 1979, he has been an Assistant Professor of Electronic Engineering at Hokkaido University. He has been engaged in research on surface acoustic waves, dielectric optical waveguides, and applications of finite-element and boundary-element methods to field problems.

Dr. Koshiba is a member of the Institute of Electronics and Communication Engineers of Japan, the Institute of Television Engineers of Japan, the Institute of Electrical Engineers of Japan, the Japan Society for Simulation Technology, and the Japan Society for Computational Methods in Engineering.

Michio Suzuki (SM'57) was born in Sapporo, Japan, on November 14, 1923. He received the B.S. and Ph.D. degrees in electrical engineering from Hokkaido University, Sapporo, Japan, in 1946 and 1960, respectively.

From 1948 to 1962, he was an Assistant Professor of Electrical Engineering at Hokkaido University. Since 1962, he has been a Professor of Electronic Engineering at Hokkaido University. From 1956 to 1957, he was a Research Associate at the Microwave Research Institute of Polytechnic Institute of Brooklyn, Brooklyn, NY.

Dr. Suzuki is a member of the Institute of Electronics and Communication Engineers of Japan, the Institute of Electrical Engineers of Japan, the Institute of Television Engineers of Japan, the Japan Society of Information and Communication Research, and the Japan Society for Simulation Technology.